

SCIENTIFIC REPORTS



OPEN

Magnetic ordering temperature of nanocrystalline Gd: enhancement of magnetic interactions via hydrogenation-induced “negative” pressure

Received: 05 November 2015

Accepted: 16 February 2016

Published: 02 March 2016

E. A. Tereshina¹, S. Khmelevskyi², G. Politova³, T. Kaminskaya⁴, H. Drulis⁵ & I. S. Tereshina^{3,4,6}

Gadolinium is a nearly ideal soft-magnetic material. However, one cannot take advantage of its properties at temperatures higher than the room temperature where Gd loses the ferromagnetic ordering. By using high-purity bulk samples with grains ~200 nm in size, we present proof-of-concept measurements of an increased Curie point (T_C) and spontaneous magnetization in Gd due to hydrogenation. From first-principles we explain increase of T_C in pure Gd due to the addition of hydrogen. We show that the interplay of the characteristic features in the electronic structure of the conduction band at the Fermi level in the high-temperature paramagnetic phase of Gd and “negative” pressure exerted by hydrogen are responsible for the observed effect.

Gadolinium, a rare earth magnet with a very high saturation polarization originating from the localized half-filled 4f-electronic shell is often regarded as an almost ideal soft-ferromagnetic material due to the small magnetic anisotropy^{1–3}. Apt for near-room-temperature magnetic refrigeration^{4–8}, the Curie temperature (T_C) of Gd hinders its application in other technological fields which require a soft magnet operating at higher temperatures. Interatomic distances affect the strength of magnetic interactions and an increase of T_C under pressure has been predicted^{9,10}. However, experimental evidence obtained on a Gd crystal under hydrostatic pressure disagrees on the direction of the Curie point shift¹¹. Therefore, a series of desirable samples can be produced by boosting the volume of Gd.

Volume expansion can be created by absorption of light elements, in particular, hydrogen. Electron bonding of hydrogen with electropositive Gd competes with a “negative” pressure exerted by hydrogenation. This may reduce the strength of the RKKY interaction and lower the T_C . Gd hydrided to low hydrogen concentrations by forming an α -GdH_x (*hcp*) solid solution preserves ferromagnetism¹². Further increasing the hydrogen content causes sequential phase transitions into antiferromagnetic β - (*fcc*, GdH₂) and γ -phases (*hcp*, GdH₃) with the ordering temperatures ~20 and 4 K, respectively. Several previous attempts to observe a hydrogen-induced Curie temperature change in coarse-grained Gd and thin films were unsuccessful^{12–14}. This is probably due to several reasons, including sample purity¹⁵ and finite size effects (for thin films). The latter are known to reduce^{16–19} the T_C significantly compared to the coarse-grained and bulk Gd. A promising result with an increased T_C was reported recently for the structurally inhomogenous α -GdH_x²⁰ consisting of needle-shaped micro-crystals embedded in nano-grained Gd matrix.

Here, we report an advance in the experimental and theoretical determination of the hydrogen-induced change of Curie temperature in Gd. We use high-purity bulk nanocrystalline, homogenous samples of Gd prepared by vacuum distillation²¹ with grains ~200 nm in size, which is then artificially doped with hydrogen. Importantly, the grains size in the studied material is not critical for the magnetic properties of Gd²². The

¹Institute of Physics CAS, 18221 Prague, Czech Republic. ²Center for Computational Materials Science, Vienna University of Technology, A-1060 Vienna, Austria. ³Baikov Institute of Metallurgy and Materials Science RAS, 119991 Moscow, Russia. ⁴Faculty of Physics, M. V. Lomonosov Moscow State University, 119991 Moscow, Russia. ⁵Institute of Low Temperature and Structure Research PAS, 50-950 Wroclaw, Poland. ⁶International Laboratory of High Magnetic Fields and Low Temperatures PAS, 53-421 Wroclaw, Poland. Correspondence and requests for materials should be addressed to E.A.T. (email: teresh@fu.cz)

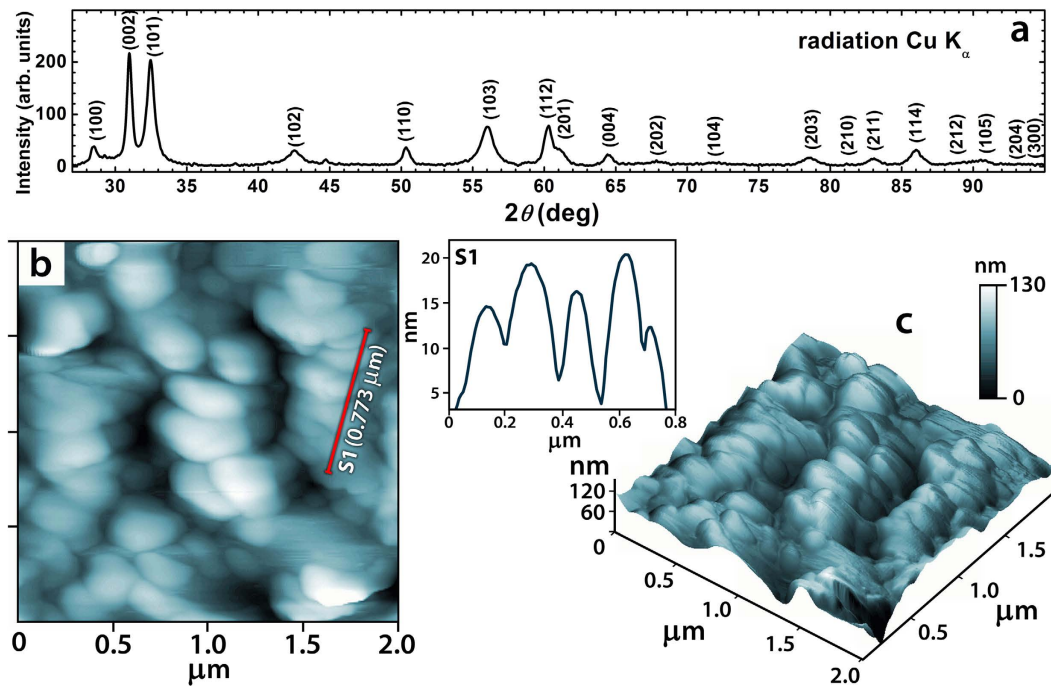


Figure 1. Room-temperature x-ray diffraction pattern of Gd (a). Typical AFM surface topography (b). Inset: (S1) cross-sectional analysis performed along the line S1 in Fig. 1 (b). Corresponding 3D surface image for distilled Gd (c).

Material	a , Å	c/a	V , Å ³	$\Delta V/V$, %		
Gd	3.633(6)	1.588(4)	65.93	–		
α -GdH _{0.22}	3.646(3)	1.586(2)	66.58	0.99		
	m' , μ_B/Gd	J_1'' , μRy	J_2'' , μRy	$T_C^{***(\text{calc})}$, K	$T_{C1}^{****(\text{exp})}$, K	$T_{C2}^{****(\text{exp})}$, K
Gd	0.459	183.2	198.6	327.9	290.8(2)	291.0(5)
α -GdH _{0.22}	0.461	183.9	199.9	332.4	296.1(2)	295.0(5)

Table 1. Structural and magnetic characteristics of Gd and α -GdH_{0.22}. m' is a local conduction band moment. The value of $7\mu_B$ from the localized $4f$ moment has to be added for the total moment. J_1'' and J_2'' are the inter-plane and in-plane exchange constants, respectively (cf. inset in Fig. 4). $T_C^{***(\text{calc})}$ is a calculated Curie temperature. $T_{C1}^{****(\text{exp})}$ and $T_{C2}^{****(\text{exp})}$ are the Curie temperatures determined using Arrott-Belov plots and the MCE maximum at $\mu_0\Delta H = 2$ T, respectively.

Arrott-Belov plot method used for determining the T_C s makes it easy to overcome unwanted thermal and magnetic field effects²³. Another method of finding the T_C is from the magnetocaloric effect (MCE) measurements. The former enables the true T_C in pure and hydrogen-charged Gd to be determined, offering a direct comparison with first principle calculations. The main purpose of the work is the determination of the physical mechanisms behind the hydrogen-induced Curie temperature enhancement in Gd.

Experimental Results and Discussion

Elemental analysis of Gd revealed the 99.99 wt.% purity with respect to other rare earth elements. The interstitial contents were determined as follows: 56 wt. ppm of C, 1 wt. ppm of N and 306 wt. ppm of O. (This is comparable or better than the sample purities in refs 24 and 25). Figure 1a shows a room-temperature x-ray diffraction pattern of the high-purity Gd. The distilled sample has an *hcp* single-phase structure and its structural characteristics (Table 1) agree well with the literature^{4,8}. The AFM (surface morphology) image obtained for this sample (piece) reveals the presence of mounds consisting of nanosized grains (Fig. 1b). The 3D-structural morphology is shown in Fig. 1c. The metal precipitation from the gaseous phase resulted in the formation of an undulating surface. The results of cross-sectional analysis performed along the line (S1) shown in Fig. 1b are presented in Fig. 1(S1). The average grain size was estimated to be 200 nm. The height difference between mounds is ranging between 20 and 80 nm.

The samples remained monolithic after exposure to hydrogen. Grains in Gd-H_x increased in size to 400–500 nm as a result of heating during the hydrogenation procedure. Yayama and Tomokiyo claimed¹² that Gd α -hydrides can be formed up to hydrogen concentrations 0.35 at.H/f.u. However, both our study and available

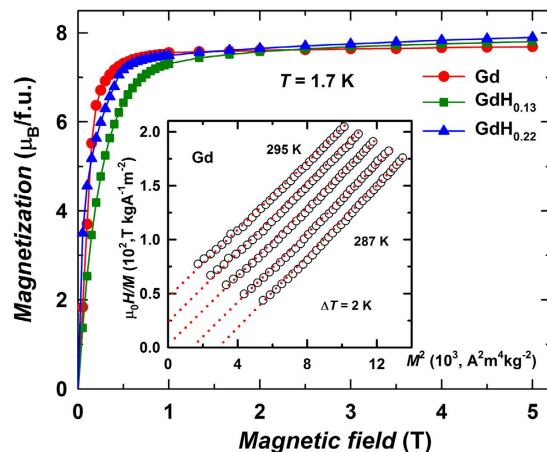


Figure 2. Field dependencies of magnetization of Gd, α -GdH_{0.13} and α -GdH_{0.22} at 1.7 K. The inset: experimental Arrott-Belov curves for Gd in the vicinity of T_C .

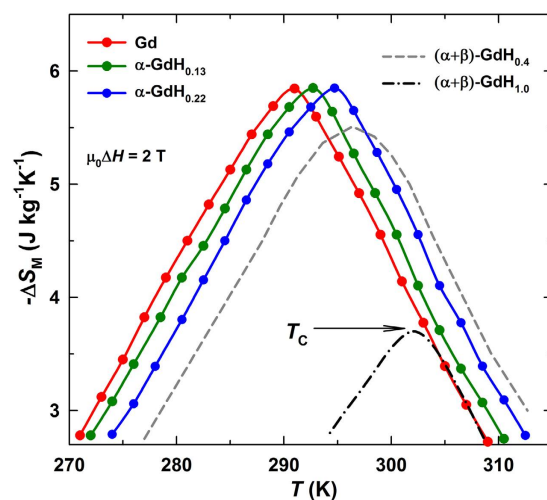


Figure 3. Magnetic entropy change ΔS_M vs. temperature for Gd, α -GdH_{0.13} and α -GdH_{0.22} at a field change of 2 T. The data for $(\alpha + \beta)$ -GdH_{0.4} and $(\alpha + \beta)$ -GdH_{1.0} are shown for comparison.

literature data¹⁴ show that it is rather difficult to avoid formation of the parasitic dihydride GdH₂ phase (β -phase) when preparing α -hydrides. Nevertheless, we succeeded in obtaining several single-phase α -GdH_x samples by optimizing (minimizing) the time of the hydrogenation procedure. The maximum hydrogen content in α -GdH_x reached 0.22 ± 0.02 at.H/f.u. (see the structural characteristics of α -GdH_{0.22} in Table 1). The structural studies of parent and hydrided samples were carried out under similar conditions so that the increase of the unit cell volume $\Delta V/V \sim 1\%$ upon hydrogenation has been found for α -GdH_{0.22}. We also obtained samples with higher hydrogen concentrations of up to 1 at.H/f.u. These, however, contained traces of the β -phase.

Figure 2 shows the M vs. H curves for Gd and α -GdH_x in fields up to 5 T at 1.7 K. A small increase of spontaneous magnetization M_s observed in α -GdH_x is in line with theoretical calculations presented below. Note that most reports on lattice-expanded Gd are on thin-film specimen, where the level of control (regarding the quantity of expansion) is rather limited. For thin Gd films, the saturation magnetization was found to drop with increasing unit cell size¹ (strained *hcp* phase) or when obtaining Gd in other structural modifications (*fcc*)²⁶. For a hydrogenated bulk specimen with rather large grains, strain and structural factors of thin films leading to the M_s decrease are eliminated.

The Curie temperatures of Gd and α -GdH_{0.22} were determined from the Arrott-Belov plots (inset in Fig. 2) as 290.8 ± 0.2 K and 296.1 ± 0.2 K, respectively (Table 1). Another method of finding the T_C is by following the maximum of the magnetocaloric effect (MCE). The magnetic entropy change, ΔS_{mag} , corresponding to the magnetic field change from zero to 2 T was calculated from the magnetization isotherms using the Maxwell relation for parent Gd and Gd-H_x (Fig. 3). This method defines the T_C in Gd and α -GdH_{0.22} as 291.0 ± 0.5 K and 295.0 ± 0.5 K, respectively. The highest observed T_C is 302.0 ± 0.5 K in $(\alpha + \beta)$ -GdH_{1.0}. Importantly, the maximum MCE in pure Gd is 5.84 J/kg·K. This is comparable with that of a Gd single crystal^{4,24}. The MCE of α -GdH_x remains of the

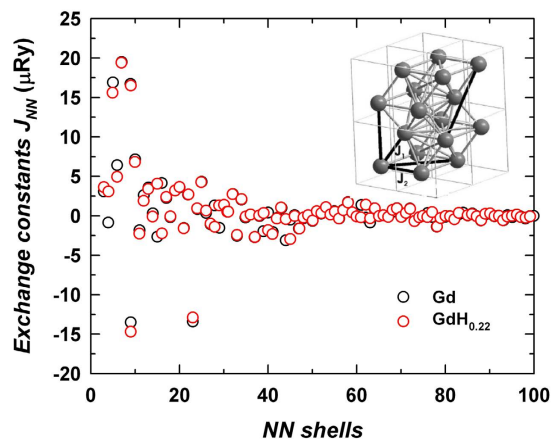


Figure 4. Calculated distant (starting from the third nearest neighbor) exchange interactions J_{NN} for Gd and GdH_{0.22}. The inset: Hexagonal crystal structure of Gd and the first two nearest-neighbor exchange interactions J_1 and J_2 .

same order of magnitude as in parent Gd while MCE in $(\alpha + \beta)$ -GdH_x gradually decreases due to the increasing content (21 and 50% for $x = 0.4$ and 1.0, respectively) of the non-magnetic at this temperature β -phase.

For Gd (and other rare earths) finite-size effects become critical upon lowering dimensions below 10 nm²². The T_C of nanostructured Gd prepared by a method similar to ours begins to decrease for crystallites smaller than 140 nm¹⁶. We find that T_C of distilled Gd is similar to single crystals^{24,27}. It stems from rather large grains ~200 nm, making the impact of finite size effects negligible. As reviewed by Dan'kov *et al.*²⁴, experimentally observed T_C s may vary depending on the purity of the studied single crystal and on the method used to determine the T_C . Below-Arrott plots used to locate T_C from $M(H)$ data allow us to determine unambiguously the increase of T_C upon hydriding high purity Gd.

Theoretical analysis and conclusions

In order to explore the physical mechanisms behind the hydrogen-induced Curie temperature enhancement in Gd, we performed first-principle calculations. Magnetic exchange constants of the Heisenberg type Hamiltonian were found using a magnetic force theorem²⁸ embedded²⁹ in Korringa-Kohn-Rostokker band structure method³⁰ within the framework of the Local Spin Density Approximation³¹. In our calculations, the c/a ratio of the *hcp* structure was fixed at values of experimental Gd and GdH_{0.22} (Table 1) while the unit cell volume was varied in order to mimic the effect of various negative chemical pressure induced by hydrogenation. The approach used for calculation is similar to that of ref. 32 performed for pure Gd in fixed lattice geometry: spin-polarized open core treatment of the Gd 4*f*-states and an *spd*-basis for the conduction band. The *spd*-valence band was calculated using a basis function expansion up to $l_{\max} = 3$ and an Atomic Sphere Approximation. The band structure calculations were converged with 14950 k -points and a convergence of exchange constants was achieved by integrating over 341595 k -points in the full Brillouine zone of a hexagonal lattice.

The local character of the 4*f*-electron moments, the very small magnetic anisotropy as well as crystal field effects due to the half-filled 4*f*-shell (zero total angular momentum) make pure *hcp* Gd a good Heisenberg system. To calculate exchange constants J_{ij} of the Hamiltonian

$$H = - \sum_{i,j \in \{Gd\}} J_{ij} \vec{e}_i \vec{e}_j \quad (1)$$

where \vec{e}_i is the unit directional vector at the i -th Gd lattice site, the conventional Disordered Local Moment (DLM) approximation³² was used to model the electronic structure in the paramagnetic state. The use of DLM allows taking into account³³ the renormalization of pair-wise exchange interactions at finite temperatures originating from the electronic structure changes in the conduction band and induced by thermal magnetic disorder of the 4*f* moments. The absolute T_C value was derived in the mean field approximation from $k_B T_C = 3/2 J_0$, where the total effective exchange constant J_0 is a sum of J_{ij} s linking a given lattice site to the remaining sites, $J_0 = \sum_i J_{oi}$.

The Curie temperatures, $T_C^{(\text{calc})}$ of Gd and GdH_{0.22} converged to the values given in Table 1 after accounting for exchange interaction constants through up to 100 nearest-neighbor (NN) shells. Table 1 also shows local conduction band moments, m , induced at the Gd atomic sites. (Note that in addition, Gd³⁺ ion has a localized moment of 7 μ_B). Two of the strongest NN interactions, inter-plane J_1 and in-plane J_2 exchange constants (inset in Fig. 4), are also shown in Table 1. The values differ from each other due to deviations from an ideal *hcp* lattice. The remaining exchange constants J_{NN} (Fig. 4) are an order of magnitude smaller.

The difference between the T_C s of pure Gd and GdH_{0.22}, 4.5 K, is in excellent agreement with experimental data. Remarkably, the overall increase of T_C is caused by long-distance interactions beyond the 20NN shells, while the first 20NN shells give less than a 1 K increase. The increase of exchange interactions due to volume expansion may look contra-intuitive when viewing the magnetic interactions in pure Gd entirely in terms of a simple RKKY model, in which the volume expansion driving the atoms farther may reduce the interaction strength. However,

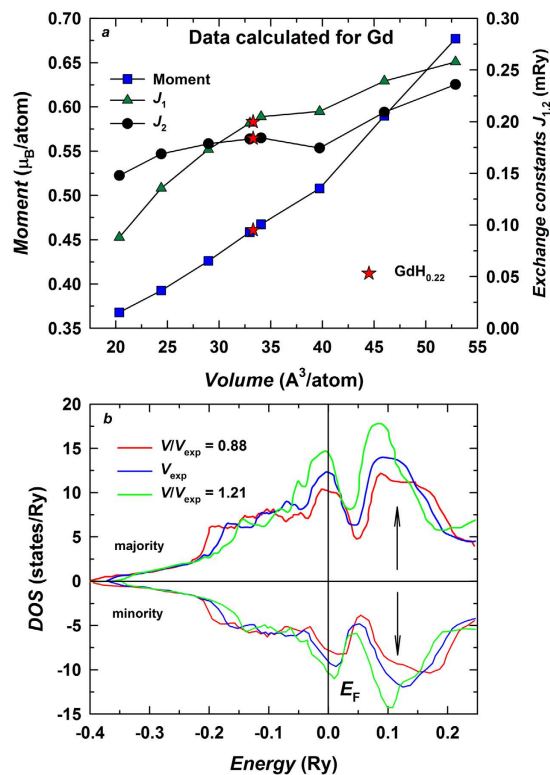


Figure 5. (a) The unit cell volume variation of conduction band moments and J_1 and J_2 exchange interactions in Gd and $\text{GdH}_{0.22}$. (b) DOS for the majority and minority spin-channels of Gd conduction band in the paramagnetic state obtained by DLM approximation using three different volumes V/V_{exp} .

the T_C change due to the volume increase can be readily understood by examining changes in the electronic structure of the Gd conduction band. To clarify this point, we expose the results of DLM calculations performed for different unit cell volumes in Fig. 5a. We present exemplary results for the c/a ratio fixed at the experimental value for pure Gd since the calculation performed for the experimental c/a ratio of $\text{GdH}_{0.22}$ does not produce any visible changes in the figure. As the unit cell of Gd expands, the induced conduction band moments in the paramagnetic state increase. This leads to the increase of the Hamiltonian's exchange constants (Eq. 1). However, the moment's increase is not the only volume-related effect which causes enhancement of the distant interactions². Another consequence of the volume expansion is the increased Density of States (DOS) of the conduction band at the Fermi level E_F (see Fig. 5b for different volumes V/V_{exp} with the experimental V_{exp} value for parent Gd). Since the long distance magnetic interaction between the $4f$ moments is mediated by conduction electrons, the increase of DOS at E_F increases the T_C .

Photoemission experiments^{34,35} showed that the conduction band of Gd retains local spin-polarization in the paramagnetic state, and the situation is far from a simple rigid-band Stoner-like picture. This feature can be promptly captured using a DLM approximation for pure Gd. Our calculations reveal two major competing forces in the paramagnetic state, namely, local spin-polarization of the conduction band arising due to the exchange interaction with the localized $4f$ shell and the band effects resulting from hybridization with neighboring sites. The latter tend to reduce spin-splitting of the majority and minority spin channels³⁶. The effect is demonstrated in Fig. 5b. Spin-splitting of the majority and minority spin-channels is indeed small, and nearly all local spin polarization is due to redistribution of spectral weight caused by the exchange interaction with the local $4f$ -moments. Hybridization decreases as the volume increases, and the conduction band becomes narrower (Fig. 5b). Both DOS at the Fermi level and local spin-polarization of the conduction band consequently increase.

To summarize, the Curie temperature increase upon hydriding is a purely electronic effect related to the expanded Gd lattice. The latter is also responsible for the small increase of spontaneous magnetization in $\alpha\text{-GdH}_x$. The use of high-purity bulk parent sample with grains ~ 200 nm in size eliminates difficulties related to the observation of this effect in thin films. It can be suggested that, irrespective of the particular manipulation used, volume increase may grant higher efficiency to Gd as a soft magnetic material.

Methods

Sample preparation and characterization. The parent Gd sample was prepared by vacuum distillation into solid phase from commercially available Gd metal (GdM-1 Grade). The metal was hydrided using a Sievert-type apparatus. Hydrogen content in the samples was found volumetrically, i.e. by measuring the pressure in the hydrogenation chamber before and after the reaction. The crystal structure of the samples was characterized by x-ray diffraction (XRD). The XRD patterns were recorded at a 0.02° scanning step on a Rigaku Ultima IV

diffractometer (Japan) with a Cu- $K\alpha$ radiation. The patterns were analyzed using a program PDXL by Rigaku integrated with the international database ICDD. Surface topology was investigated by an atomic force microscopy in a semi contact mode using the SMENA-A scanning electron microscope mounted on a Solver platform (NT-MDT) at ambient conditions. A high-precision silicon HA_{NC} probe (10 nm curvature tip radius) with an Au reflective side was used for the study (force constant 3.5 N/m and a nominal resonant frequency of 129.4 kHz).

Magnetic study. The samples magnetization $M(H)$ was measured on rod-shaped samples (length 5–7 mm, diameter 0.1–0.2 mm) using a PPMS-14 magnetometer (Quantum Design, USA) at a constant field step (0.05 T) and at various temperatures (2 K step). The Curie temperatures of the parent and hydrided Gd were determined by means of the Arrott-Belov plot method based on the thermodynamic theory²³. The accuracy of the Arrott-Belov's method is the highest among other techniques for the T_C determination. It has a standard experimental error of ± 0.2 K. The second method used to evaluate the T_C is by detecting the maximum of magnetocaloric effect. In the present work, the MCE was studied by measuring the magnetization $M(H)$ at a field change from zero to 2 T. The magnetic entropy change ΔS_m was calculated using the Maxwell relation.

References

- Scheunert, G. *et al.* Influence of strain and polycrystalline ordering on magnetic properties of high moment rare earth metals and alloys. *J. Phys. D: Appl. Phys.* **47**, 415005 (2015).
- Oroszlany, L. *et al.* Magnetism of Gadolinium: A First-Principles Perspective. *Phys. Rev. Lett.* **115**, 096402 (2015).
- Jensen, J. & Mackintosh, A. *Rare Earth Magnetism: Structures and Excitations* (Clarendon Press, Oxford, 1991).
- Tishin, A. M. & Spichkin, Y. I. The magnetocaloric effect and its application (eds Coey, J. M. D. *et al.*) 401–417 (Institute of Physics Publishing, Bristol, 2003).
- Gschneidner, K. A. Jr., Pecharsky, V. K. & Tsokol, A. O. Recent developments in magnetocaloric materials. *Rep. Prog. Phys.* **68**, 1479–1539 (2005).
- Kitanovski, A. *et al.* Magnetocaloric Energy Conversion - From Theory to Applications, 269–327 (Springer International Publishing, Switzerland, 2015).
- He, X. N. *et al.* Design and performance of a room-temperature hybrid magnetic refrigerator combined with Stirling gas refrigeration effect. *Int. J. Refrigeration* **36**, 1465–1471 (2013).
- Nikitin, S. A. *Magnetic Properties of Rare-Earth Metals and Compounds*, 187–195 (Publishing House MSU, Moscow, 1989).
- Bozorth, R. M. *Ferromagnetism* (D. Van Nostrand Company, Toronto-New York-London, 1951).
- Patrick, L. The Change of Ferromagnetic Curie Points with Hydrostatic Pressure. *Phys. Rev.* **93**, 384–392 (1954).
- Bartholin, H. & Bloch, D. Effect of a Uniaxial Stress on the Curie Temperature of a Single Crystal of Gd. *Phys. Rev.* **188**, 845–848 (1969).
- Yayama, H. & Tomokiyo, A. In *Advances in Cryogenic Engineering (Materials)* (eds Fickett, F. R. & Reed, R. P.), Vol. 38, 293–298 (Plenum Press, New York, 1992).
- Yamada, Y. *et al.* The Curie temperature dependence on preparation conditions for Gd thin films. *Thin Solid Films* **459**, 191–194 (2004).
- Cizek, J. *et al.* Defect studies of hydrogen-loaded nanocrystalline Gd films. *Appl. Surf. Sci.* **255**, 251–253 (2008).
- Gschneidner, K. A. Jr. Metals, alloys and compounds-high purities do make a difference! *J. Alloys Compd.* **193**, 1–6 (1993).
- Michels, D., Krill, C. E. & Birringer, R. Grain-size-dependent Curie transition in nanocrystalline Gd: the influence of interface stress. *J. Magn. Magn. Mater.* **250**, 203–211 (2002).
- Mathew, S. P. *et al.* Magnetic irreversibility, spin-wave excitations and magnetocaloric effect in nanocrystalline Gadolinium. *J. Phys. Conf. Series* **200**, 072047 (2010).
- Hsu, C.-J. *et al.* Magnetic anisotropy in nanostructured gadolinium, *J. Appl. Phys.* **111**, 053916 (2012).
- Paschen, U., Surgers, C. & Vonlohneysen, H. Magnetic properties of thin epitaxial Gd films on Nb. *Z. Phys. B* **90**, 289–296 (1993).
- Burkhanov, G. S. *et al.* Magnetocaloric properties of distilled gadolinium: Effects of structural inhomogeneity and hydrogen impurity. *Appl. Phys. Lett.* **104**, 242402(5) (2014).
- Devyatykh, G. G. & Burkhanov, G. S. *High-purity refractory and rare-earth metals* (Cambridge: Intern. Sci. Publ., 1997).
- O'Shea, M. J. & Perera, P. Influence of nanostructure (layers and particles) on the magnetism of rare-earth materials. *J. Appl. Phys.* **85**, 4322 (1999).
- Zverev, V. I. *et al.* The role of demagnetization factor in determining the 'true' value of the Curie temperature. *J. Magn. Magn. Mater.* **323**, 2453–2457 (2011).
- Dan'kov, S. Y. *et al.* Magnetic phase transitions and the magnetothermal properties of gadolinium. *Phys. Rev. B* **57**, 3478–3490 (1998).
- Lyubina, J. *et al.* Magnetic field dependence of the maximum magnetic entropy change. *Phys. Rev. B* **83**, 012403(4) (2011).
- Bertelli, T. P. *et al.* Ferromagnetic properties of fcc Gd thin films. *J. Appl. Phys.* **117**, 203904 (2015).
- Coey, J. M. D., Skumryev, V. & Gallagher, K. Is gadolinium really ferromagnetic? *Nature* **401**, 35 (1999).
- Liechtenstein, A. I. *et al.* Local spin density functional approach to the theory of exchange interactions in ferromagnetic metals and alloys. *J. Magn. Magn. Mater.* **67**, 65–74 (1987).
- Ruban, A. V. *et al.* Local lattice relaxations in random metallic alloys: Effective tetrahedron model and supercell approach. *Phys. Rev. B* **67**, 214302 (2003).
- Ruban, A. V. & Skriver, H. L. Calculated surface segregation in transition metal alloys. *Comp. Mat. Science* **15**, 119–143 (1999).
- Perdew, J. P. *et al.* Atoms, molecules, solids, and surfaces: Applications of the generalized gradient approximation for exchange and correlation. *Phys. Rev. B* **46**, 6671–6687 (1992).
- Khmelevskiy, S. *et al.* Magnetic exchange interactions in the paramagnetic state of hcp Gd. *J. Phys.: Cond. Matter* **19**, 326218 (2007).
- Gyorfyy, B. L. *et al.* A first-principles theory of ferromagnetic phase transitions in metals. *J. Phys. F: Met. Phys.* **15**, 1337–1386 (1985).
- Maiti, K. *et al.* Electronic Band Structure of Gd: A Consistent Description. *Phys. Rev. Lett.* **86**, 2846–2849 (2001).
- Maiti, K. *et al.* Finite Temperature Magnetism in Gd: Evidence against a Stoner Behavior. *Phys. Rev. Lett.* **88**, 167205 (2002).
- Khmelevskiy, S., Turek, I. & Mohn, P. Spontaneous volume magnetostriction and non-Stoner behavior of the valence band in pure hcp Gd. *Phys. Rev. B* **70**, 132401 (2004).

Acknowledgements

We thank Prof. G. Burkhanov and O. Chistyakov for the provision of a distilled sample; A. Hackemer for the hydrogenation procedure. This work was supported by the RFBR, No. 16-03-00612 and 14-03-31342, and by the Czech Science Foundation, GACR 16-03593S. Part of the measurements has been performed in MLTL (<http://mltl.eu>) supported within the program of Czech Research Infrastructures (project no. LM2011025).

Author Contributions

E.A.T. collected and analyzed the magnetization data; S.K. performed the first principles calculations; G.P. characterized the samples and measured the MCE effect; T.K. performed the AFM study; H.D. synthesized hydrides; I.S.T. designed the study and supervised the project; E.A.T., S.K. and I.S.T. contributed equally to writing the paper. All authors contributed to the interpretation of the data and commented on the manuscript.

Additional Information

Competing financial interests: The authors declare no competing financial interests.

How to cite this article: Tereshina, E. A. *et al.* Magnetic ordering temperature of nanocrystalline Gd: enhancement of magnetic interactions via hydrogenation-induced “negative” pressure. *Sci. Rep.* **6**, 22553; doi: 10.1038/srep22553 (2016).



This work is licensed under a Creative Commons Attribution 4.0 International License. The images or other third party material in this article are included in the article's Creative Commons license, unless indicated otherwise in the credit line; if the material is not included under the Creative Commons license, users will need to obtain permission from the license holder to reproduce the material. To view a copy of this license, visit <http://creativecommons.org/licenses/by/4.0/>